Use of a genetically engineered mouse model as a preclinical tool for HER2 breast cancer

Helen Creedon[1], Lucy A Balderstone[1,5], Morwenna Muir[1], Jozef Balla[1], Laura Gomez-Cuadrado[1], Natasha Tracey[1], Joseph Loane[2], Teresa Klinowska[3], William J Muller[4], Valerie G Brunton[1]

[1]Edinburgh Cancer Research UK Centre, University of Edinburgh, Crewe Road South, Edinburgh, EH4 2XR

[2]Pathology Department, Western General Hospital, Edinburgh, EH4 2ZD

[3]AstraZeneca Oncology iMed, Alderley Park, Macclesfield, SK10 4TG

[4]Goodman Cancer Research Center, McGill University, Montreal, Canada, H3A 1A3

[5]Current address AstraZeneca Innovative Medicines & Early Development, Darwin Building, Cambridge Science Park, Cambridge, CB4 0FZ

Correspondence: Prof Valerie Brunton
    Phone: 0131 777 3556
    FAX: 0131 777 3520
    Email: v.brunton@ed.ac.uk

KEY WORDS: HER2, breast cancer, resistance, epithelial-to-mesenchymal transition

SUMMARY STATEMENT

This study demonstrates the utility of a transgenic mouse model of breast cancer to define mechanisms of resistance to a pan-HER family inhibitor and identifies a link with EMT.

ABSTRACT

Resistance to HER2 targeted therapies presents a major clinical problem. Although preclinical studies have identified a number of possible mechanisms clinical validation has been difficult. This most likely reflects the reliance on cell line models that do not recapitulate the complexity and heterogeneity seen in human tumours. Here we show the utility of a genetically engineered mouse model of HER2 driven breast cancer (MMTV-NIC) to define mechanisms of resistance to the pan-HER family inhibitor AZD8931. Genetic manipulation of MMTV-NIC mice demonstrated that loss of PTEN conferred de novo resistance to AZD8931, while a tumour fragment transplantation model was established to assess mechanisms of acquired resistance. Using this approach 50% of tumours developed resistance to AZD8931. Analysis of the resistant tumours showed two distinct patterns of resistance: tumours in which reduced membranous HER2 expression was associated with an epithelial-to-mesenchymal transition (EMT) and resistant tumours that retained HER2 expression and an epithelial morphology. The plasticity of the EMT phenotype was demonstrated upon re-implantation of resistant tumours that then showed a mixed epithelial and mesenchymal phenotype. Further AZD8931 treatment resulted in the generation of secondary resistant tumours that again had either undergone EMT or had retained their original epithelial morphology. The data provide a strong rationale for basing therapeutic decisions on the biology of the individual resistant tumour, which may be very different from that of the primary tumour and will be specific to individual patients.

INTRODUCTION

HER2 (human epidermal growth factor receptor 2) gene amplification and/or protein overexpression occurs in around 20% of breast cancers and is associated with poor prognosis. Several drugs capable of specifically targeting the HER2 pathway have been developed for use in both early and late HER2-positive disease and have had a significant impact on the treatment of HER2-positive breast cancer (Arteaga et al, 2012). These include antibodies directed against HER2 including trastuzumab and pertuzumab, and also small molecule tyrosine kinase inhibitors that target the kinase activity of HER2 and HER1 such as lapatinib. Although initial response rates to the current HER2-targeted therapies are good, resistance is inevitable. Further tyrosine kinase inhibitors including AZD8931 (sapatinib) and neratinib have been developed in an attempt to improve efficacy rates and duration of response. Preclinical studies have identified numerous mechanisms of both de novo and acquired resistance (Creedon et al, 2014; Rexer & Arteaga, 2012) although their clinical validation has been more difficult which reflects the inability of the conventional cell based approaches to adequately model the complexity of the human disease.

   The limitation of conventional cell culture and mouse xenograft studies is well recognized as an obstacle to the effective translation of preclinical findings into clinical benefit (Sharpless & Depinho, 2006). Use of genetically engineered models in which tumours develop in situ in the context of an intact microenvironment is a viable alternative for preclinical assessment of both drug response and mechanisms of resistance (van Miltenburg & Jonkers, 2012). Generation of autochthonous tumours driven by cell specific expression of oncogenic drivers or loss of tumour suppressors relevant to human tumours gives rise to tumours in which the histopathology and disease progression also recapitulate many aspects of the human disease providing more relevant models with which to study drug response. Here we describe the use of a HER2 driven model of mammary tumourigenesis as a preclinical tool to study response and resistance mechanisms in HER2-positive breast cancer. We have used the MMTV-NIC (Neu-IRES-Cre) model (Ursini-Siegel et al, 2008), which employs a bicistronic transcript to co-express activated ErbB2/Neu (HER2) with MMTV-Cre recombinase, resulting in the formation of activated ErbB2/Neu driven mammary tumours. The advantage of this model is that the coupling of activated ErbB2/Neu with Cre recombinase in the same cell means that Cre negative tumour cells are not generated allowing the efficient Cre-mediated deletion of additional conditional

alleles (Schade et al, 2009). This allows validation of potential mechanisms of de novo resistance such as loss of PTEN. Loss of PTEN and subsequent activation of the PI3K pathway has been identified as a key determinant of trastuzumab sensitivity and has been associated with poorer overall survival in trastuzumab treated patients (Berns et al, 2007; Esteva et al, 2010; Nagata et al, 2004) although the impact on lapatinib resistance remains unclear (Xia et al, 2007). Here we have coupled loss of PTEN with HER2 activation in the MMTV-NIC model and demonstrate that loss of PTEN is associated with de novo resistance to the small molecule tyrosine kinase inhibitor sapatinib (AZD8931). We also show the utility of the model for identifying mechanisms of acquired resistance to HER2 targeted therapy and identify the induction of an epithelial-to-mesenchymal transition (EMT) in a sub-population of AZD8931 resistant tumours.

RESULTS

Loss of PTEN confers resistance to AZD8931

Initial experiments were carried out to determine whether the MMTV-NIC model was sensitive to the HER family tyrosine kinase inhibitor AZD8931. As loss of PTEN and activation of the PI3K signaling pathway has previously been reported to confer resistance to trastuzumab, cohorts of both MMTV-NIC PTEN^{+/+} and MMTV-NIC PTEN^{+/-} mice were used. Both MMTV-NIC PTEN^{+/+} and MMTV-NIC PTEN^{+/-} mice developed on average 4 tumours per mouse with 100% penetrance. As described previously, loss of PTEN accelerated tumour onset in the MMTV-NIC mice (Schade et al, 2009). The median age of tumour onset was 102 days in the MMTV-NIC PTEN^{+/-} cohort compared to 150 days in the MMTV-NIC PTEN^{+/+} cohort (p=0.0001, Gehan-Breslow-Wilcoxon test)(Supplementary Fig. 1A). Western blot analysis of tumours showed reduced expression of PTEN and increased phosphorylation of Akt in tumours taken from the MMTV-NIC PTEN^{+/-} mice consistent with increased signaling through the PI3K pathway (Supplementary Fig. 1B).

To assess the response to AZD8931, we randomized cohorts of MMTV-NIC PTEN^{+/+} and MMTV-NIC PTEN^{+/-} mice to treatment with either AZD8931 or vehicle. Median survival in the vehicle arm of the MMTV-NIC PTEN^{+/+} cohort following the start of treatment was 35 days (range 10-39 days), compared with 18 days (range 11-24 days) in vehicle treated MMTV-NIC PTEN^{+/-} mice. Drug treatment was stopped at 40 days when all vehicle treated animals were sacrificed due to tumour burden. At this time none of the drug treated animals had to be sacrificed due to tumour burden (Fig. 1A and B). When we looked at the growth of the individual index tumours (defined as the largest tumour at the time of sacrifice) in the different cohorts after 40 days, we saw that all AZD8931 treated MMTV-NIC PTEN^{+/+} tumours initially responded to treatment and 2 out of 5 tumours fully resolved. The growth of a further 2 tumours was inhibited while the final tumour initially responded but after 17 days of drug treatment became insensitive and after 40 days of treatment, its volume had increased by 134.2%. By comparison, the tumours in the vehicle treated arm continued to grow throughout the experiment and the median percentage change in tumour volume was an increase of 294.6% (Fig. 1C). By contrast, all but 1 of 5 AZD8931 treated MMTV-NIC PTEN^{+/-} tumours became rapidly insensitive to AZD8931 and by day 40 all AZD8931 treated tumours had grown beyond their initial starting volume with a median percentage change in tumour volume of 131.1%. As

expected, all vehicle-treated tumours continued to grow steadily throughout the experiment with a median percentage change in tumour volume of 415.1% (Fig. 1D). In summary, AZD8931 resulted in tumour shrinkage in the majority of MMTV-NIC PTEN$^{+/+}$ animals but whilst it slowed tumour growth in MMTV-NIC PTEN$^{+/-}$ animals it did not cause tumour resolution. We also noted that by day 40 there were fewer additional tumours in both the MMTV-NIC PTEN$^{+/+}$ and MMTV-NIC PTEN$^{+/-}$ animals treated with AZD8931 and although this did not reach statistical significance the reduction in tumour burden was greater in the MMTV-NIC PTEN$^{+/+}$ mice, consistent with the increased sensitivity of the MMTV-NIC PTEN$^{+/+}$ tumours to AZD8931 (median values for tumours per mouse were: MMTV-NIC PTEN$^{+/+}$, vehicle=5; MMTV-NIC PTEN$^{+/+}$, AZD8931=1; MMTV-NIC PTEN$^{+/-}$, vehicle=6; MMTV-NIC PTEN$^{+/-}$, AZD8931=3, p=0.1025, Kruskal-Wallis). This illustrates the significant heterogeneity in response to AZD8931 between the two different cohorts and demonstrates that loss of PTEN leading to activation of the PI3K pathway confers de novo resistance to AZD8931.

As there was little residual tissue from the AZD8931 treated MMTV-NIC PTEN$^{+/+}$ animals at the completion of the experiment, additional cohorts of both MMTV-NIC PTEN$^{+/+}$ and MMTV-NIC PTEN$^{+/-}$ mice were treated with vehicle or AZD8931 for 3 days and effects on HER family signaling pathways assessed. There was a reduction in phosphorylation of HER2 and HER3 in MMTV-NIC PTEN$^{+/+}$ and MMTV-NIC PTEN$^{+/-}$ tumours following treatment with AZD8931 compared to vehicle treated animals although this did not reach statistical significance following histoscoring (Fig. 1E). This reflects the heterogenous expression and activation of both HER2 and HER3 in the tumours (Supplementary Fig. 1C). No significant EGFR (HER1) expression was detected in the MMTV-NIC tumours so it was not possible to assess effects on EGFR activation (results not shown). We used reverse phase protein arrays to look at downstream signaling to Akt, MAPK and S6 in the AZD8931 treated tumours and found that their activation was significantly inhibited in MMTV-NIC PTEN$^{+/+}$ and MMTV-NIC PTEN$^{+/-}$ tumours (Fig. 1F). Immunohistochemical analysis showed that pAkt was confined to the tumour cells and not expressed in the surrounding stroma, while pMAPK was also expressed in the stroma and the reduced expression of pMAPK may therefore also reflect reduced activation of MAPK in the surrounding stroma (Supplementary Fig. 1D). Thus short-term treatment with AZD8931 treatment inhibits HER family signaling in both tumour types and the

differential response of the MMTV-NIC PTEN$^{+/+}$ and MMTV-NIC PTEN$^{+/-}$ tumours does therefore not reflect an inability of the drug to inhibit the target in the different tumours.

Establishment of orthotopic transplanted tumours

The multifocal nature of the MMTV-NIC model means that it is not possible to study mechanisms of acquired drug resistance. We therefore established whether the MMTV-NIC PTEN tumours could be orthotopically transplanted into syngeneic wild type FVB/N mice to provide a more tractable model for drug resistance studies. We were able to establish tumours following transplantation of tumour fragments from MMTV-NIC PTEN$^{+/-}$ tumours but not from MMTV-NIC PTEN$^{+/+}$ tumour fragments. Examination of H&E sections from the fragment derived MMTV-NIC PTEN$^{+/-}$ tumours confirmed the presence of highly mitotic, grade 3 carcinomas, which were indistinguishable from tumours that developed in the parental MMTV-NIC PTEN$^{+/-}$ model (Fig. 2A). Both parental and fragment derived tumours demonstrated inter-and intra-tumoural heterogeneity in HER2 expression (Fig. 2B) and consistent with the frequent observation of mitotic figures on H&E sections, a high percentage of nuclei stained positively for Ki67 in both parental and fragment derived tumours (Fig. 2C). The orthotopic transplantation model therefore provides a useful tool by circumventing problems associated with the multifocal nature of the genetically engineered model.

Initial studies to determine the suitability of the MMTV-NIC transplantation model for drug efficacy studies were carried out using the taxane paclitaxel whose role in the management of both early and metastatic breast cancer is well established (Gajria et al, 2010; Ghersi et al, 2005). Paclitaxel treatment resulted in a statistically significant increase in overall survival of mice bearing fragment-derived tumours. Median overall survival was increased from 14 days in vehicle treated animals (range 7-14 days) to 24 days (range 24-24 days) in drug treated animals (p=0.03, Gehan-Breslow Wilcoxon test). Looking at the response of individual tumours to treatment, we found that although paclitaxel slowed tumour growth, it did not result in tumour shrinkage (Fig. 2D).

Development of resistance to AZD8931

We next determined whether the MMTV-NIC tumours could be used to model acquired resistance to AZD8931. We generated tumour fragments from 3 separate MMTV-NIC PTEN^{+/-} donor mice. From each, donor tumour fragments were then transplanted into cohorts of 6 wild type FVB/N mice. Following the development of established tumours, mice were randomized to treatment with either vehicle (n=3) or AZD8931 (n=3). AZD8931 treatment resulted in an initial inhibition of tumour growth in all mice. When tumours had regressed to $\leq 0.1 cm^3$, AZD8931 treatment was stopped: following the subsequent regrowth of the tumour, treatment was then re-started when tumours reached $\geq 0.3 cm^3$. This cycle was repeated until tumours either resolved or became resistant where they were able to continue growing in the presence of ongoing treatment. The resistant tumours originated from different donors and the treatment duration required for the individual tumours to become resistant varied between individual tumours (Fig. 3A).

Histopathological examination of the matched AZD8931 naïve and resistant tumours revealed that although all the AZD8931 naïve tumours were histologically indistinguishable from each other (Fig. 3B, C) there were significant differences in the AZD8931 resistant tumours (Fig. 3D, E). While some of the resistant tumours had the same histopathological phenotype as their matched naïve tumour (Fig. 3D), a sub-set of resistant tumours had a more pleomorphic appearance and were comprised of spindle cells suggestive of tumours under going EMT (Fig. 3E).

Loss of cell surface E-cadherin is an established marker of EMT and while strong membranous expression of E-cadherin was seen in all drug naïve tumours, loss of E-cadherin in the resistant tumours was associated with the conversion to a spindle cell morphology (Fig. 4A-D), with the resistant tumours that had not undergone the morphological change retaining expression of E-cadherin (Fig. 4I-L). This loss of E-cadherin was accompanied by expression of the mesenchymal marker vimentin in the resistant spindle cell tumours (Fig. 4E, F) indicating that these resistant tumours have undergone EMT. HER2 expression was preserved in the resistant tumours which had retained the histopathological features of the drug naïve tumours (Fig. 4O, P), but total loss of membranous HER2 expression was seen in the resistant spindle cell tumours (Fig. 4G, H).

To establish whether the resistant phenotype was stable, fragments from one individual resistant tumour were reimplanted into cohorts of wild type FVB/N mice.

Following the development of established tumours, mice were randomized to treatment with either vehicle or AZD8931. AZD8931 treatment prevented the growth of one tumour, although tumour regression did not occur (Fig. 5A, red growth curve, "AZD8931 responsive"). The remaining three tumours responded initially to AZD8931, although resistance did develop over time (Fig. 5A, black growth curves, "AZD8931 resistant"). The onset of secondary resistance was faster than in the orginal drug naïve tumour fragments (compare Figs 3A, 5A).

The vehicle treated tumours were all highly mitotic with rounded cells with pleomorphic nuclei (Fig. 5B). The tumour whose growth was inhibited by AZD8931 had mild to moderately pleomorphic nuclei and no mitoses (Fig. 5C). The resistant tumours had distinct morphologies: two of the tumours were comprised of highly mitotic spindle cells with similar histology to those seen in the primary resistant tumours that had undergone EMT (compare Fig. 5E, F and Fig. 3C), while the remaining resistant tumour had a papillary architecture with moderate/marked nuclear pleomorphism (Fig. 5D). As we had previously demonstrated a reduction in pAkt and pMAPK following acute treatment with AZD8931 (Fig. 1F) we looked at activation of Akt and MAPK following development of resistance to AZD8931 (Fig. 6G-P). Chronic exposure to AZD8931 did not reduce pAkt and pMAPK levels, although one AZD89231 resistant tumour showed an overall reduction in pMAPK staining with only small pockets of pMAPK positive cells scattered throughout the tumour (Fig. 6N).

Further analysis of the tumours revealed that all vehicle treated tumours expressed both E-cadherin and vimentin (Fig. 6A). The AZD8931 responsive tumour was also both E-cadherin and vimentin positive although the number of vimentin positive tumour cells was much lower than in the vehicle treated tumours (Fig. 6B). As with the primary resistant tumours the two spindle cell AZD8931 resistant tumours had lost E-cadherin and were strongly vimentin positive. Strikingly this was associated with loss of membranous HER2 expression (Fig. 6D, E). The remaining AZD8931 resistant tumour resembled the vehicle treated tumours being both E-cadherin and vimentin positive (Fig. 6C). Thus the development of resistance to AZD8931 in a sub-population of tumours is linked to increased expression of markers associated with the induction of EMT and loss of membranous HER2. To further explore the mechanisms of EMT induction in the resistant tumours we looked at expression of Zeb1 which is a known transcriptional regulator of EMT. Upregulation of nuclear Zeb1 was only seen in the resistant spindle cell tumours consitent with a Zeb1 regulated induction of EMT (Fig. 7).

DISCUSSION

It is widely acknowledged that the use of conventional xenograft models for preclinical drug testing has limited predictive clinical value. Use of genetically engineered mouse models provides a useful alternative in which drug response and resistance can be evaluated in situations that more faithfully recapitulate the human disease (Olive et al, 2009; Singh et al, 2010; Wang et al, 2012). Here we show that the MMTV-NIC model has utility in assessing efficacy and resistance mechanisms of HER2 targeted therapies. Comparison of tumours with the same genotype demonstrated heterogeneity in the rate and extent of response to AZD8931, despite the use of predefined genetic mutations to drive tumour development. This variation in therapeutic response has been previously described in other genetically engineered models (Rottenberg et al, 2007) and contrasts with the more uniform response seen in xenograft studies (Becher & Holland, 2006). This is an important advance as it enables us to more accurately recapitulate the behaviour of human tumours and is most likely due to the random acquisition of secondary mutations during tumour development and progression in these models. In addition we show for the first time that acquired resistance to a HER2 targeted therapy can be modeled in MMTV-NIC tumours. The majority of studies exploring resistance to HER2 directed therapies have used cell line based approaches and although numerous resistance mechanisms have been identified in vitro, clinical validation has proved challenging. The use of genetically engineered models to explore resistance mechanisms offers a more physiologically relevant system with tumours developing resistance whilst exposed to ongoing in vivo selection pressures. Therefore any resistance strategies identified may be more predictive of clinically relevant resistance mechanisms.

We identified PTEN loss as an important determinant of de novo AZD8931 resistance. Loss of PTEN and subsequent activation of the PI3K pathway has been identified as a key determinant of trastuzumab sensitivity and has been associated with poorer overall survival in trastuzumab treated patients (Berns et al, 2007; Esteva et al, 2010; Nagata et al, 2004) although the impact on lapatinib resistance remains unclear (Xia et al, 2007). Like lapatinib, AZD8931 is a dual inhibitor of both HER2 and HER1, however, it has a unique profile of activity being a more effective inhibitor of HER family signaling than lapatinib resulting in a distinct profile of anti-tumour activity (Hickinson et al, 2010). Current trials are underway to determine

whether the more effective simultaneous inhibition of HER family signaling provided by AZD8931 could have clinical benefit (Tjulandin et al, 2013), and thus understanding potential mechanisms of resistance to AZD8931 is required. Both MMTV-NIC PTEN$^{+/+}$ and MMTV-NIC PTEN$^{+/-}$ tumours displayed reduced Akt activity following treatment with AZD8931, although in both models there was still evidence of residual activity following AZD8931 treatment. Incomplete inhibition of Akt signaling is a well-established mechanism of resistance to HER2 targeted therapies (Rexer & Arteaga, 2012) and is likely to contribute to the continued tumour progression in the MMTV-NIC PTEN$^{+/-}$ model. In support of this we saw no reduction in pAkt in AZD8931 MMTV-NIC PTEN$^{+/-}$ resistant tumours following chronic drug treatment. Other studies have shown that combination therapy using a HER2 monoclonal antibody and an Akt inhibitor inhibited growth of MMTV-NIC PTEN$^{-/-}$ tumours, which were resistant to treatment with either drug alone (Wang et al, 2012). Taken together this supports the use of Akt inhibitors in combination with HER2 targeted therapies and a number of clinical trials are currently underway to evaluate the use of trastuzumab and/or lapatinib with Akt inhibitors.

One of the major advantages of using the MMTV-NIC tumours for modeling drug resistance was the generation of resistant tumours with distinct molecular phenotypes, which recapitulates in part the heterogeneity seen in the clinic. This provides a strong rationale for basing therapeutic decisions on the biology of the individual resistant tumour, which may be very different from that of the primary tumour. For example, the observation that a sub-set of our resistant tumours no longer expressed high levels of membranous HER2 could have a significant impact on future treatments. To date, major advances in overcoming clinical resistance to trastuzumab have focused on alternative strategies for targeting HER2 signaling, either through combining drugs which target different HER family receptors or through use of drug-antibody conjugates such as trastuzumab-emtansine. As it is rarely mandatory to re-biopsy tumours at the time of entry into clinical trials, patients whose tumours no longer express HER2 risk being exposed to the toxicity of treatments that might not be anticipated to be effective.

Several in vitro studies have shown that resistance to lapatinib and trastuzumab are associated with induction of EMT (Creedon et al, 2014; Kim et al, 2013; Korkaya et al, 2012; Oliveras-Ferraros et al, 2012) and our finding that a sub-set of the resistant tumours have undergone EMT indicates that targeting pathways that regulate EMT

may be effective in a sub-population of resistant tumours (Singh & Settleman, 2010). Interestingly the generation of mixed vimentin and E-cadherin positive tumours following re-implantation of an AZD8931 resistant tumour shows that the induction of EMT is not binary and that the tumours are highly plastic and can respond to microenvironmental factors that can affect their EMT status. The initial response of the re-implanted resistant tumour fragments to AZD8931 most likely reflects this plasticity with the reversion to a more epithelial phenotype and the concomitant re-expression of HER2 conferring initial drug sensitivity. Although we have shown that the induction of EMT is associated with acquired resistance to AZD8931, induction of EMT in HER2-driven mouse mammary tumours via expression of an activating PI3K mutation was associated with de novo resistance to HER2 targeted therapies (Hanker et al, 2013) while in vitro studies showed that expression of transcription factors that drive EMT was causally related to de novo trastuzumab resistance (Oliveras-Ferraros et al, 2012).

One of the main challenges going forward is the identification of effective drug combinations to combat resistance to HER2 targeted therapies. Use of the transplantable tumour model described here provides a powerful preclinical tool with which to test potential novel combinations in resistant tumours, studies which to date rely on use of resistant cell lines established in vitro. For example, exploiting the molecular differences in resistant tumours that have undergone EMT may provide alternative combination strategies for overcoming resistance in these tumours.

MATERIALS AND METHODS

Animals

MMTV-NIC mice expressing an oncogenic ErbB2/Neu allele and Cre recombinase under the control of the MMTV promoter were generated as previously described (Ursini-Siegel et al, 2008) and inter-crossed with floxed *Pten* (strain C;129S4-*Pten^{tm1Hwu}*/J, Jackson Laboratory) mice to generate either MMTV-NIC PTEN$^{+/+}$ or MMTV-NIC PTEN$^{+/-}$ progeny on a FVB/N background. Genotyping was carried out by Transnetyx (Cordova, TN, USA). All experiments were conducted in compliance with UK Home Office guidelines. Nulliparous females were monitored twice weekly, using manual palpation, for tumour formation. The greatest tumour dimension and its perpendicular measurement were recorded and once tumours had reached their maximum size (1.5 cm in one direction) as determined by Home Office regulations, mice were sacrificed. Tumours were then collected and fixed in 10% neutral buffered formalin. Tumours used for the generation of fragments were washed in ice cold PBS and cut into 1 mm^3 fragments and any macroscopic necrotic areas removed and then centrifuged at 450g for 1 minute. The supernatant, containing fibrous and necrotic material, was removed and the remaining fragments suspended in cryopreservation buffer (50% DMEM, 45% foetal bovine serum, 5% DMSO) and stored at -80^{0}C. At the time of transplantation, fragments were defrosted at room temperature, washed in PBS and inserted into the fourth mammary fat pad.

For drug studies using AZD8931 (AstraZeneca Oncology iMed, Alderley Park, UK) treatment was commenced when mice had at least 1 tumour $\geq$ 0.1 cm^3 (index tumour) and continued until complete resolution of the index tumour or until the animal was sacrificed due to tumour size $\geq$ 1.5 cm (in any direction). Mice were dosed daily with vehicle 1% Tween 80 (in PBS) or AZD8931 (100 mg/kg) suspended in 1% Tween 80 (in PBS) by oral gavage. To generate tumours that were resistant to AZD8931 an intermittent drug treatment schedule was performed. Following transplantation of tumour fragments tumours were allowed to grow to $\geq$ 0.1 cm^3 before treatment with AZD8931 as above was started. When tumours regressed to < 0.1 cm^3, AZD8931 treatment was stopped and tumours monitored twice weekly. If the tumour regrew treatment was then re-started when tumours reached $\geq$ 0.3 cm^3. This cycle was repeated until tumours developed resistance and were sacrificed when the maximum tumour size (1.5 cm in any direction) was reached as permitted under UK Home Office regulations. For drug studies using paclitaxel, treatment was

commenced when mice had at least 1 tumour ≥ 0.15 cm^3 (index tumour) and continued until the animal was sacrificed due to tumour size or when the experiment was terminated 72 hours after the fourth dose of paclitaxel. Mice were dosed weekly with vehicle (cremaphor EL:ethanol, 1:1, v:v) or paclitaxel (10 mg/kg) suspended in cremaphor EL:ethanol by intraperitoneal injection.

Immunohistochemistry

Immunohistochemistry of formalin-fixed, paraffin-embedded tissues was performed as described previously (Karim et al, 2013). Primary antibodies used were HER2 (Invitrogen, Cat#AHO1011, 1:1000), pY1221/1222 HER2 (Cat#2243, 1:400), pY1289 HER3 (Cat#4791, 1:100), Ki67 (Vector, Cat#VP-RM04, 1:500), E-cadherin (Cat#3195, 1:5000), vimentin (Cat#5741, 1:100), pS473 Akt (Cat#4060, 1:50) and pT202/Y204 MAPK (Cat#4370, 1:400)(all Cell Signaling, UK).

Western blotting

Western blot analysis was performed as described previously (Karim et al, 2013). Primary antibodies used were HER2 (Cat#2248, 1:1000), pS473 Akt (Cat#4060, 1:1000), Akt (Cat#9272, 1:1000), PTEN (Cat#9552, 1:1000) and (all Cell Signaling, UK) and β-actin (Cat#A4700, Sigma, UK; 1:5000).

Reverse phase protein array (RPPA) analysis

Tumours were washed with PBS and lysed in 1% Triton X-100, 50 mM HEPES (pH 7.4), 150 mM sodium chloride, 1.5 mM magnesium chloride, 1 mM EGTA, 100 mM sodium fluoride, 10 mM sodium pyrophosphate, 1 mM sodium vanadate, 10% glycerol, supplemented with cOmplete ULTRA protease inhibitor and PhosSTOP phosphatase inhibitor cocktails (Sigma, UK). Cleared lysates were serially diluted to produce a dilution series comprising four serial two-fold dilutions of each sample, which were spotted onto nitrocellulose-coated slides (Grace Bio-Labs, supplied by Sigma, UK) in triplicate under conditions of constant 70% humidity using the Aushon 2470 array platform (Aushon Biosystems, Billerica, MA, USA). Slides were hydrated in blocking buffer (Thermo Fisher Scientific, UK) and then incubated with primary antibodies (all 1:250 from Cell Signaling, UK). Bound antibodies were detected by

incubation with anti-rabbit DyLight 800-conjugated secondary antibody (New England BioLabs, UK). An InnoScan 710-IR scanner (Innopsys, Carbonne, France) was used to read the slides, and images were acquired at the highest gain without saturation of the fluorescence signal. The relative fluorescence intensity of each sample replicate was quantified using Mapix software (Innopsys).

The linear fit of the dilution series of each sample was determined for each primary antibody, from which median relative fluorescence intensities were calculated, and samples with $R^2 < 0.8$ in all three replicates were excluded. Signal intensities were normalized by global sample median normalization (Guo et al, 2012).

Author contributions

H.C., L.A.B., M.M., J.B. N.T. and L.G.C. carried out the experiments and analysed the data. J.L. carried out the histological evaluation and contributed to writing the manuscript. T.K. provided intellectual input and contributed to writing the manuscript. W.J.M. provided the mouse lines and intellectual input. H.C. and V.G.B. conceived and designed the experiments and wrote the manuscript.

Competing interests

T.K. and L.A.B. are employees of AstraZeneca. All other authors have no competing interests.

References

Arteaga CL, Sliwkowski MX, Osborne CK, Perez EA, Puglisi F, Gianni L (2012) Treatment of HER2-positive breast cancer: current status and future perspectives. *Nat Rev Clin Oncol* **9:** 16-32

Becher OJ, Holland EC (2006) Genetically engineered models have advantages over xenografts for preclinical studies. *Cancer Res* **66:** 3355-3358

Berns K, Horlings HM, Hennessy BT, Madiredjo M, Hijmans EM, Beelen K, Linn SC, Gonzalez-Angulo AM, Stemke-Hale K, Hauptmann M, Beijersbergen RL, Mills GB, van de Vijver MJ, Bernards R (2007) A functional genetic approach identifies the PI3K pathway as a major determinant of trastuzumab resistance in breast cancer. *Cancer Cell* **12:** 395-402

Creedon H, Byron A, Main J, Hayward L, Klinowska T, Brunton VG (2014) Exploring mechanisms of acquired resistance to HER2 (human epidermal growth factor receptor 2)-targeted therapies in breast cancer. *Biochem Soc Trans* **42:** 822-830

Esteva FJ, Guo H, Zhang S, Santa-Maria C, Stone S, Lanchbury JS, Sahin AA, Hortobagyi GN, Yu D (2010) PTEN, PIK3CA, p-AKT, and p-p70S6K status: association with trastuzumab response and survival in patients with HER2-positive metastatic breast cancer. *Am J Pathol* **177:** 1647-1656

Gajria D, Seidman A, Dang C (2010) Adjuvant taxanes: more to the story. *Clin Breast Cancer* **10 Suppl 2:** S41-49

Ghersi D, Wilcken N, Simes RJ (2005) A systematic review of taxane-containing regimens for metastatic breast cancer. *Br J Cancer* **93:** 293-301

Guo H, Liu W, Ju Z, Tamboli P, Jonasch E, Mills GB, Lu Y, Hennessy BT, Tsavachidou D (2012) An efficient procedure for protein extraction from formalin-fixed, paraffin-embedded tissues for reverse phase protein arrays. *Proteome Sci* **10:** 56

Hanker AB, Pfefferle AD, Balko JM, Kuba MG, Young CD, Sanchez V, Sutton CR, Cheng H, Perou CM, Zhao JJ, Cook RS, Arteaga CL (2013) Mutant PIK3CA accelerates HER2-driven transgenic mammary tumors and induces resistance to combinations of anti-HER2 therapies. *Proc Natl Acad Sci U S A* **110:** 14372-14377

Hickinson DM, Klinowska T, Speake G, Vincent J, Trigwell C, Anderton J, Beck S, Marshall G, Davenport S, Callis R, Mills E, Grosios K, Smith P, Barlaam B, Wilkinson RW, Ogilvie D (2010) AZD8931, an equipotent, reversible inhibitor of signaling by epidermal growth factor receptor, ERBB2 (HER2), and ERBB3: a unique agent for simultaneous ERBB receptor blockade in cancer. *Clin Cancer Res* **16:** 1159-1169

Karim SA, Creedon H, Patel H, Carragher NO, Morton JP, Muller WJ, Evans TR, Gusterson B, Sansom OJ, Brunton VG (2013) Dasatinib inhibits mammary tumour development in a genetically engineered mouse model. *J Pathol* **230:** 430-440

Kim HP, Han SW, Song SH, Jeong EG, Lee MY, Hwang D, Im SA, Bang YJ, Kim TY (2013) Testican-1-mediated epithelial-mesenchymal transition signaling confers acquired resistance to lapatinib in HER2-positive gastric cancer. *Oncogene* **33:** 3334-3341

Korkaya H, Kim GI, Davis A, Malik F, Henry NL, Ithimakin S, Quraishi AA, Tawakkol N, D'Angelo R, Paulson AK, Chung S, Luther T, Paholak HJ, Liu S, Hassan KA, Zen Q, Clouthier SG, Wicha MS (2012) Activation of an IL6 inflammatory loop mediates trastuzumab resistance in HER2+ breast cancer by expanding the cancer stem cell population. *Mol Cell* **47:** 570-584

Nagata Y, Lan KH, Zhou X, Tan M, Esteva FJ, Sahin AA, Klos KS, Li P, Monia BP, Nguyen NT, Hortobagyi GN, Hung MC, Yu D (2004) PTEN activation contributes to tumor inhibition by trastuzumab, and loss of PTEN predicts trastuzumab resistance in patients. *Cancer Cell* **6:** 117-127

Olive KP, Jacobetz MA, Davidson CJ, Gopinathan A, McIntyre D, Honess D, Madhu B, Goldgraben MA, Caldwell ME, Allard D, Frese KK, Denicola G, Feig C, Combs C, Winter SP, Ireland-Zecchini H, Reichelt S, Howat WJ, Chang A, Dhara M, Wang L, Ruckert F, Grutzmann R, Pilarsky C, Izeradjene K, Hingorani SR, Huang P, Davies SE, Plunkett W, Egorin M, Hruban RH, Whitebread N, McGovern K, Adams J, Iacobuzio-Donahue C, Griffiths J, Tuveson DA (2009) Inhibition of Hedgehog signaling enhances delivery of chemotherapy in a mouse model of pancreatic cancer. *Science* **324:** 1457-1461

Oliveras-Ferraros C, Corominas-Faja B, Cufi S, Vazquez-Martin A, Martin-Castillo B, Iglesias JM, Lopez-Bonet E, Martin AG, Menendez JA (2012) Epithelial-to-mesenchymal transition (EMT) confers primary resistance to trastuzumab (Herceptin). *Cell Cycle* **11:** 4020-4032

Rexer BN, Arteaga CL (2012) Intrinsic and acquired resistance to HER2-targeted therapies in HER2 gene-amplified breast cancer: mechanisms and clinical implications. *Crit Rev Oncog* **17:** 1-16

Rottenberg S, Nygren AO, Pajic M, van Leeuwen FW, van der Heijden I, van de Wetering K, Liu X, de Visser KE, Gilhuijs KG, van Tellingen O, Schouten JP, Jonkers J, Borst P (2007) Selective induction of chemotherapy resistance of mammary tumors in a conditional mouse model for hereditary breast cancer. *Proc Natl Acad Sci U S A* **104:** 12117-12122

Schade B, Rao T, Dourdin N, Lesurf R, Hallett M, Cardiff RD, Muller WJ (2009) PTEN deficiency in a luminal ErbB-2 mouse model results in dramatic acceleration of mammary tumorigenesis and metastasis. *J Biol Chem* **284:** 19018-19026

Sharpless NE, Depinho RA (2006) The mighty mouse: genetically engineered mouse models in cancer drug development. *Nat Rev Drug Discov* **5:** 741-754

Singh A, Settleman J (2010) EMT, cancer stem cells and drug resistance: an emerging axis of evil in the war on cancer. *Oncogene* **29:** 4741-4751

Singh M, Lima A, Molina R, Hamilton P, Clermont AC, Devasthali V, Thompson JD, Cheng JH, Bou Reslan H, Ho CC, Cao TC, Lee CV, Nannini MA, Fuh G, Carano RA, Koeppen H, Yu RX, Forrest WF, Plowman GD, Johnson L (2010) Assessing therapeutic responses in Kras mutant cancers using genetically engineered mouse models. *Nature Biotech* **28:** 585-593

Tjulandin S, Moiseyenko V, Semiglazov V, Manikhas G, Learoyd M, Saunders A, Stuart M, Keilholz U (2013) Phase I, dose-finding study of AZD8931, an inhibitor of EGFR (erbB1), HER2 (erbB2) and HER3 (erbB3) signaling, in patients with advanced solid tumors. *Invest New Drugs*

Ursini-Siegel J, Hardy WR, Zuo D, Lam SH, Sanguin-Gendreau V, Cardiff RD, Pawson T, Muller WJ (2008) ShcA signalling is essential for tumour progression in mouse models of human breast cancer. *EMBO J* **27:** 910-920

van Miltenburg MH, Jonkers J (2012) Using genetically engineered mouse models to validate candidate cancer genes and test new therapeutic approaches. *Curr Opin Genet Dev* **22:** 21-27

Wang Q, Li SH, Wang H, Xiao Y, Sahin O, Brady SW, Li P, Ge H, Jaffee EM, Muller WJ, Hortobagyi GN, Yu D (2012) Concomitant targeting of tumor cells and induction of T-cell response synergizes to effectively inhibit trastuzumab-resistant breast cancer. *Cancer Res* **72:** 4417-4428

Xia W, Husain I, Liu L, Bacus S, Saini S, Spohn J, Pry K, Westlund R, Stein SH, Spector NL (2007) Lapatinib antitumor activity is not dependent upon phosphatase and tensin homologue deleted on chromosome 10 in ErbB2-overexpressing breast cancers. *Cancer Res* **67:** 1170-1175

Figures
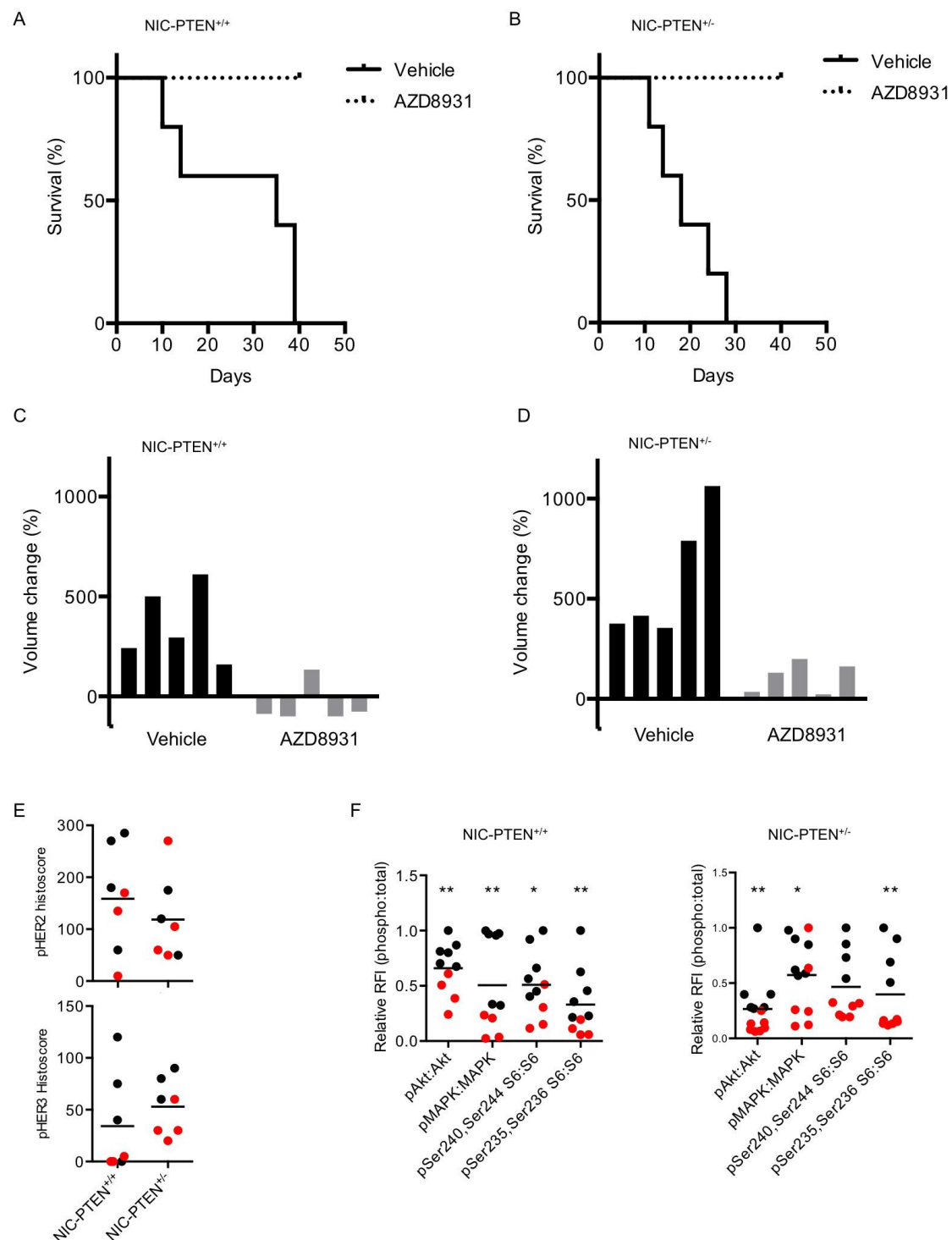
Fig. 1: PTEN status determines the sensitivity to AZD8931. Cohorts of MMTV-NIC-PTEN$^{+/+}$ and NIC-PTEN$^{+/-}$ mice were randomized to treatment with daily AZD8931 or vehicle and tumour response monitored. (A) Overall survival in vehicle

(n=5) and AZD8931 (n=5) treated NIC-PTEN$^{+/+}$ mice (p=0.0043, Gehan-Breslow Wilcoxon test). (B) Overall survival in vehicle (n=5) and AZD8931 (n=5) treated NIC-PTEN$^{+/-}$ mice (p=0.0039, Gehan-Breslow Wilcoxon test). (C) Waterfall plot of percentage tumour volume change over duration of experiment in NIC-PTEN$^{+/+}$ vehicle and AZD8931 treated animals (p=0.0079, Mann Whitney U test). (D) Waterfall plot of percentage tumour volume change over duration of experiment in NIC-PTEN$^{+/-}$ vehicle and AZD8931 treated animals (p=0.0079, Mann Whitney U test). Vehicle treated mice were sacrificed when tumour burden reached maximum permitted size: 10-39 days for MMTV-NIC PTEN$^{+/+}$ mice) and 11-24 days for MMTV-NIC PTEN$^{+/-}$ mice. AZD8931 treatment was stopped at 40 days when all vehicle treated animals were sacrificed due to tumour burden. (E) Immunohistochemical analysis was performed on paraffin embedded sections of AZD8931 and vehicle treated tumours with pTyr 1221/1222 HER2 and pTyr 1289 HER3 antibodies. Membranous histoscore calculated as the sum of the product of percentage cells stained by the intensity graded from 0-3, where 1=weak, 2=moderate and 3=strong staining (histoscore = (% *1) + (% *2) + (% *3)). pTyr 1221/1222 HER2 staining NIC-PTEN$^{+/+}$: p=0.48, NIC-PTEN$^{+/-}$: p=1.0 and pTyr1289 HER3 staining NIC-PTEN$^{+/+}$: p=0.20, NIC-PTEN$^{+/-}$: p=0.07 Mann-Whitney U test comparing vehicle and AZD8931 treated tumours. Black data points represent vehicle treated tumours. Red data points represent AZD8931 treated tumours. Bar represent mean value for each genotype. (F) Reverse phase protein array analysis was performed on lysate from AZD8931 (red data points) and vehicle (black data points) treated NIC-PTEN$^{+/+}$ and NIC-PTEN$^{+/-}$ tumours. The ratio of phospho:total protein RFI value is presented and normalized to the maximum value in each data set. *p≤0.05 and **p≤0.01 comparing vehicle and AZD8931 for each antibody, Mann Whitney U test.
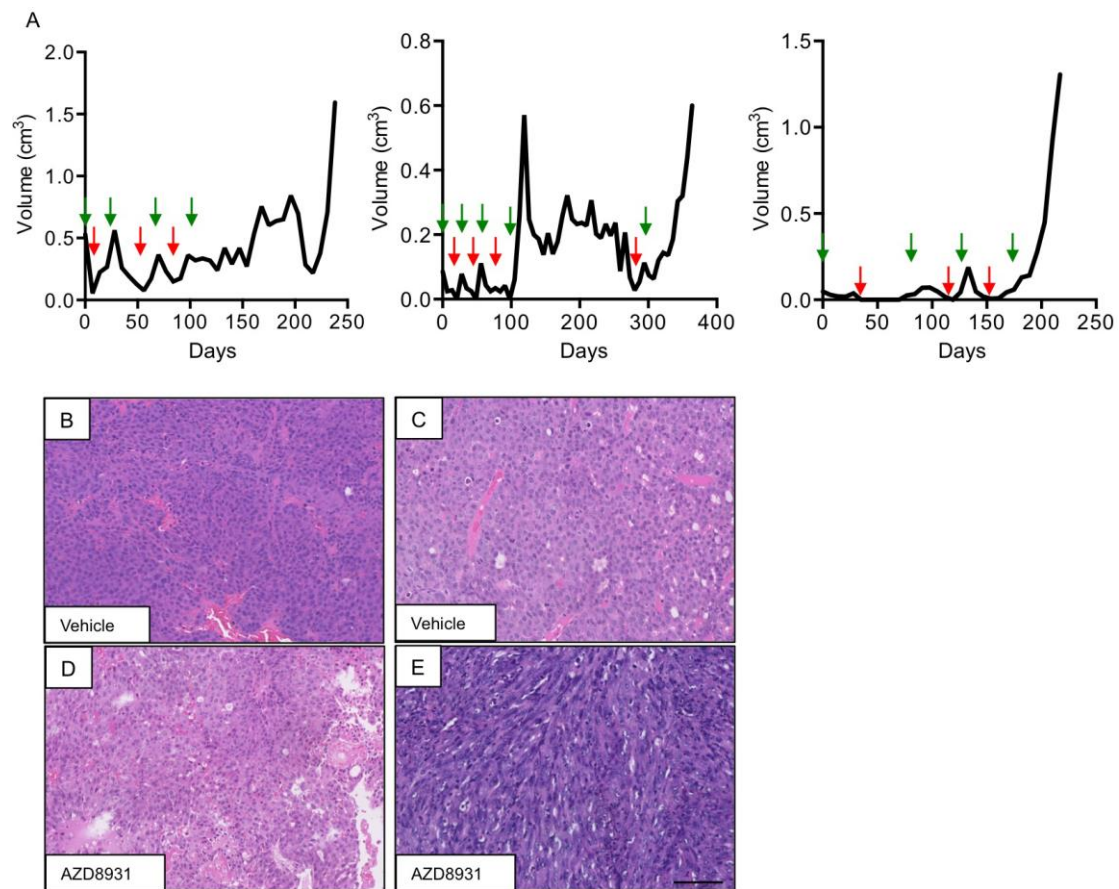
Fragment derived tumour   Spontaneous tumour

H&E

HER2

Ki67

D
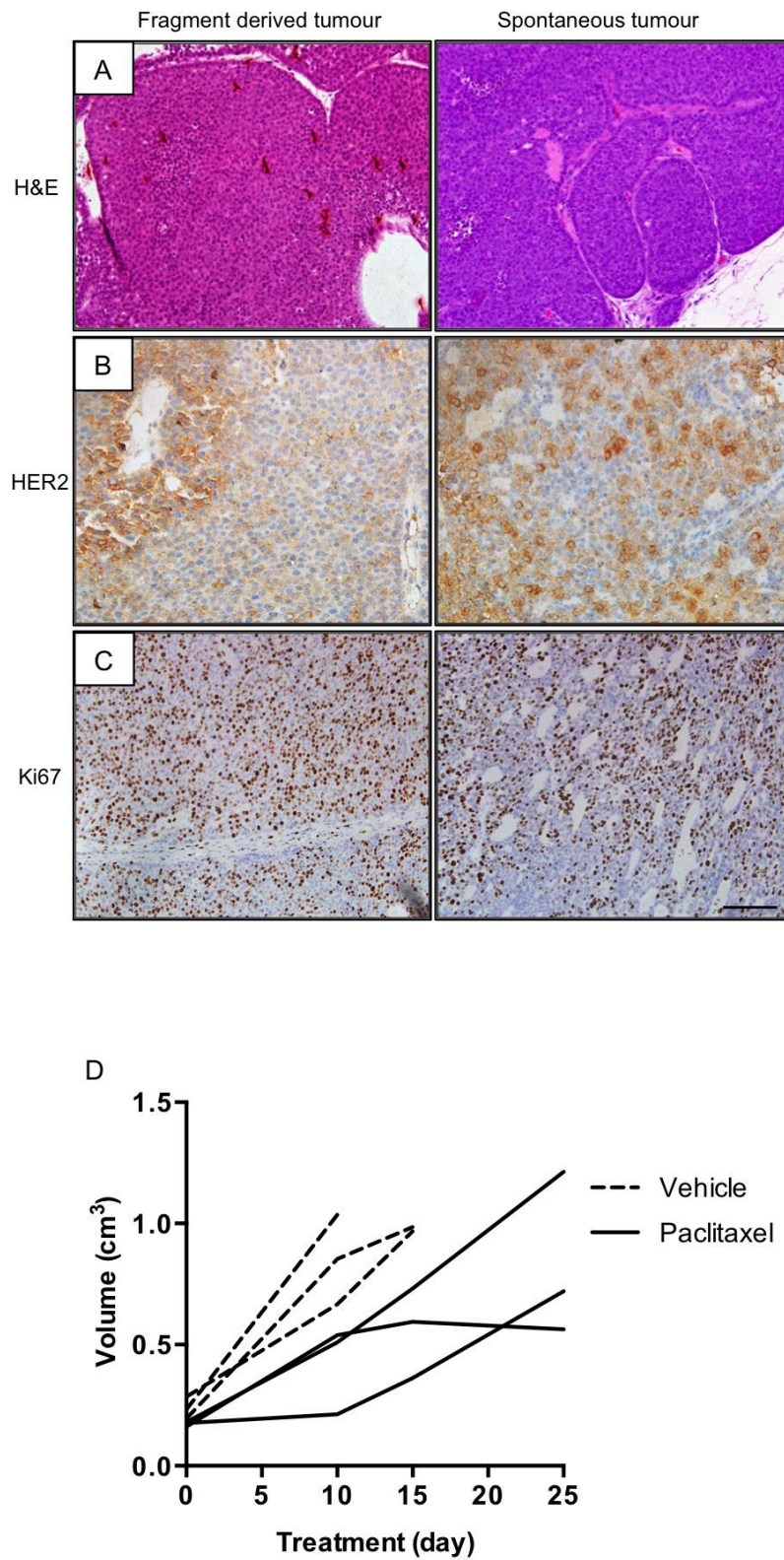
Fig. 2: Transplantation of NIC-PTEN$^{+/-}$ fragments generated tumours that were indistinguishable from the parental tumours. (A) Representative H&E images of

fragment derived and spontaneous tumours from NIC-PTEN$^{+/-}$ mice. Mag x20. (B) Representative images of HER2 and (C) Ki67 expression in fragment derived and spontaneous tumours. Mag x20, scale bar 100 μm. (D) Growth rate of vehicle (n=3) and paclitaxel (n=3) treated fragment derived tumours.

Fig. 3: Generation of fragment derived tumours with acquired resistance to AZD8931. (A) Representative growth curves of 3 independent NIC-PTEN^{+/-} tumour fragments treated with AZD8931. Repeated cycles of AZD8931 were administered to facilitate the selection of tumours with acquired resistance to AZD8931. Green arrowheads indicate the start of treatment and red arrowheads indicate when treatment was stopped. (B, C) Representative H&E images of AZD8931 naïve (vehicle) and resistant tumours. (D) AZD8931 resistant tumour phenotypically indistinguishable from AZD8931 naive tumour. (E) AZD8931 resistant tumours consisted of spindle shaped cells. Mag x20, scale bar 100 μm.
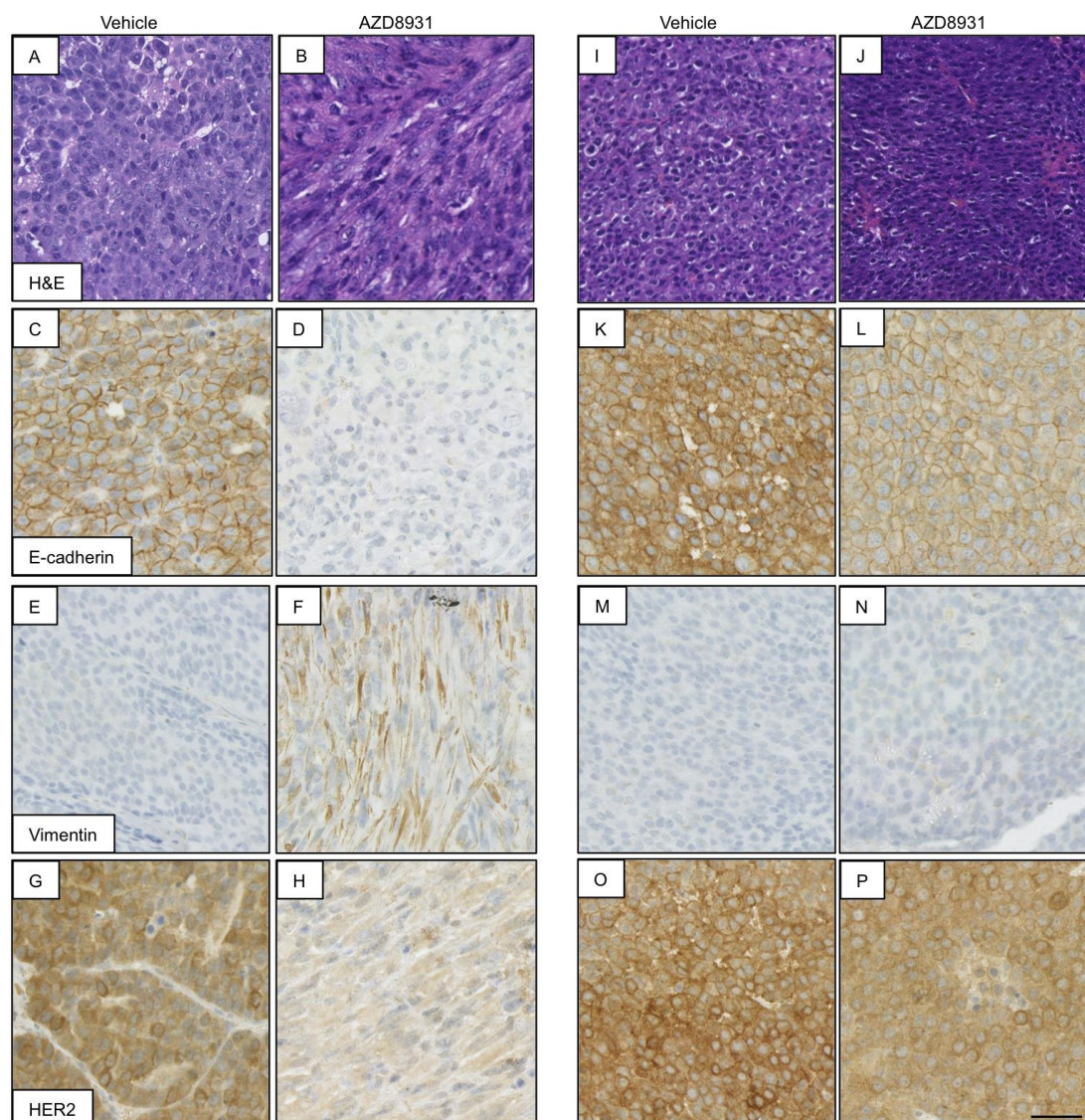
Fig. 4: AZD8931 resistance is associated with EMT in a sub-population of tumours. Analysis of AZD8931 naive (vehicle) and resistant tumours showing representative images of H&E staining and immunohistochemical analysis of E-cadherin, vimentin and HER2. Mag x20, scale bar 50 μm. (A-H) AZD8931 resistant spindle cell tumour and corresponding vehicle treated tumour. (I-P) AZD8931 resistant tumour phenotypically indistinguishable from AZD8931 naïve (vehicle) tumour and corresponding vehicle treated tumour.
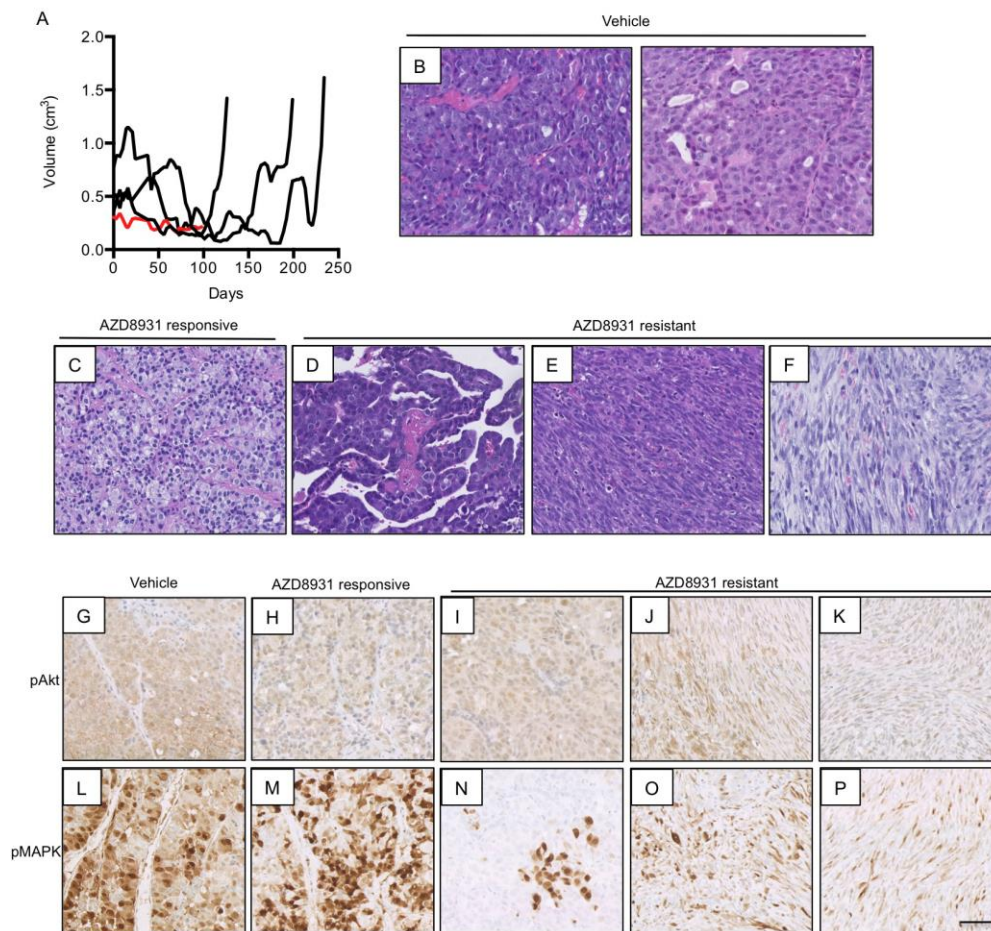
Fig. 5: Generation of secondary resistance in NIC-PTEN$^{+/-}$ tumour fragments.
(A) Growth curves of NIC-PTEN$^{+/-}$ AZD8931 resistant tumour fragments following treatment with repeated cycles of AZD8931. Black lines represent tumours that developed resistance to AZD8931. Red line represents tumour whose growth was inhibited by AZD8931. Treatment was stopped after 90 days due to lack of tumour growth. (B) Representative H&E staining of vehicle treated tumours. (C-F) H&E staining of AZD8931 treated tumours: (C) shows AZD8931 responsive tumour (red line in (A)) whose growth was inhibited by AZD893, (D) shows resistant tumour that has retained the morphology of the AZD8931 naïve (vehicle) tumours an (E, F) show resistant tumours with a spindle cell morphology. (G-P) Immunohistochemical analysis of pAkt (G-K) and pMAPK (L-P) in vehicle and AZD8931 treated tumours. Mag x20, scale bar 50 μm.
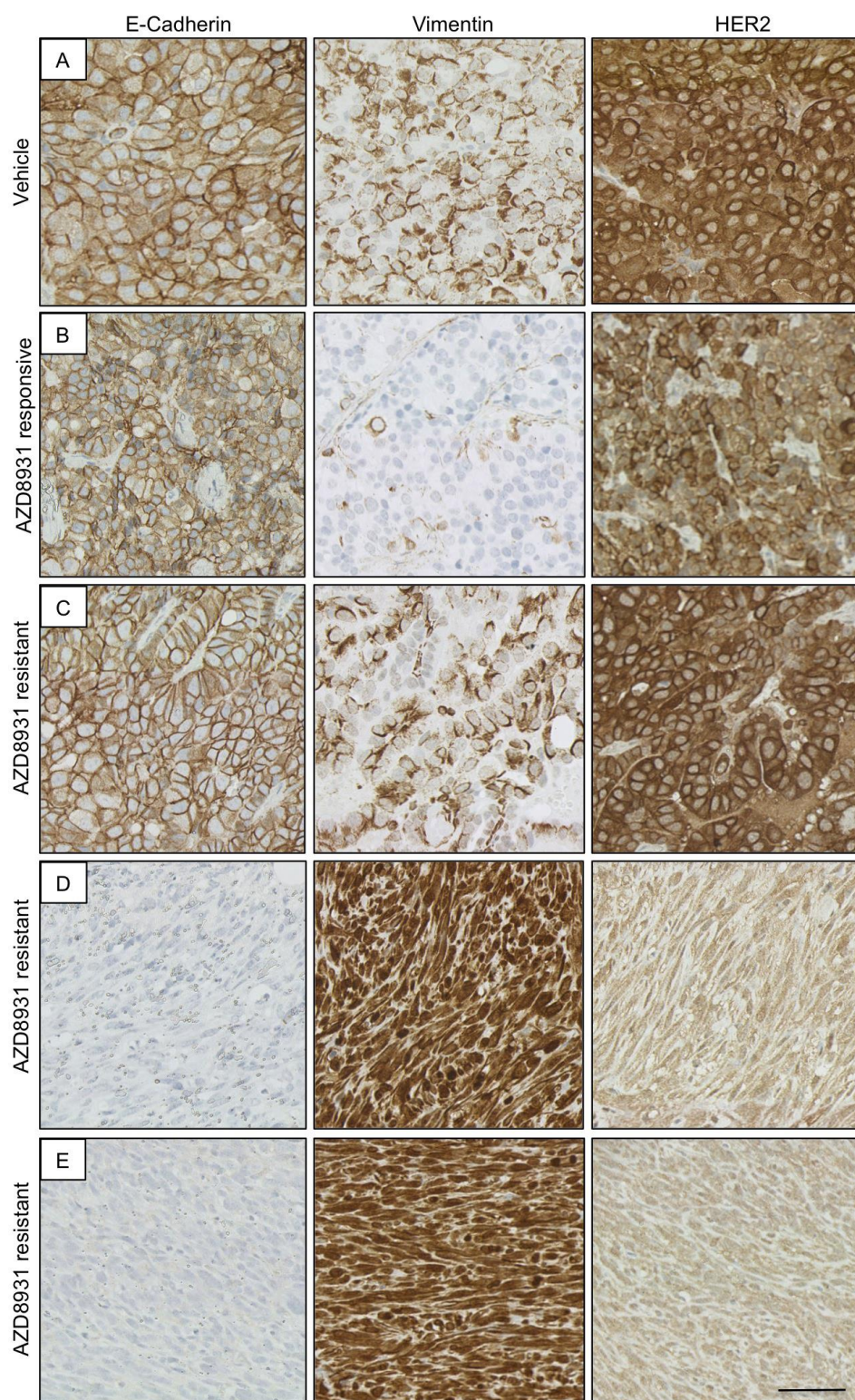
Fig. 6: Development of EMT in AZD8931 resistant tumours.
Immunohistochemical analysis of E-cadherin, vimentin and HER2 in (A) vehicle and

(B-E) AZD8931 treated tumours. (B) Shows AZD8931 responsive tumour whose growth was inhibited by AZD8931, (C) shows resistant tumour that has retained the morphology of the AZD8931 naïve (vehicle) tumours and (D, E) show resistant tumours with a spindle cell morphology. Mag x20, scale bar 50 μm.
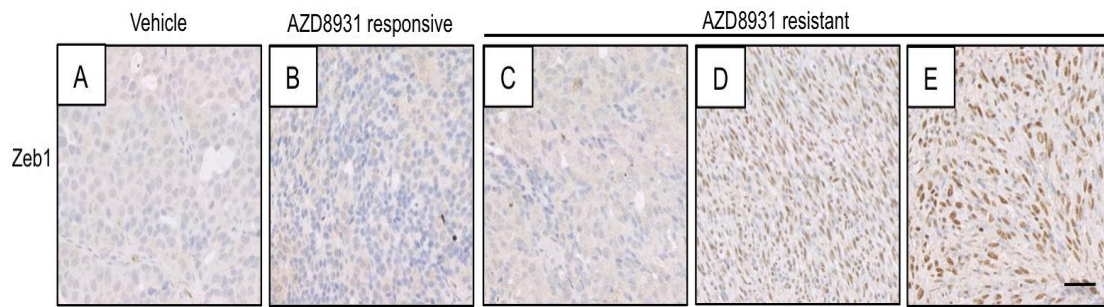
Fig. 7: Nuclear Zeb1 expression in spindle cell resistant tumours. Immunohistochemical analysis of Zeb1 in (A) vehicle and (B-E) AZD8931 treated tumours. (B) Shows AZD8931 responsive tumour whose growth was inhibited by AZD8931, (C) shows resistant tumour that has retained the morphology of the AZD8931 naïve (vehicle) tumours and (D, E) show resistant tumours with a spindle cell morphology. Mag x20, scale bar 50 μm.

TRANSLATIONAL IMPACT

Clinical issue

HER2 (human epidermal growth factor receptor 2) gene amplification and/or protein overexpression occurs in around 20% of breast cancers and is associated with poor prognosis. Several drugs capable of specifically targeting the HER2 pathway have been developed for use in both early and late HER2-positive disease and have had a significant impact on the treatment of HER2-positive breast cancer. However both de novo and acquired resistance is a major clinical problem with the use of these agents. Preclinical studies have identified numerous mechanisms of both de novo and acquired resistance although their clinical validation has been more difficult. This reflects the inability of conventional cell based approaches to adequately model the complexity of the human disease. The use of genetically engineered mouse models driven by relevant oncogenes and/or tumour suppressors in which the histopathology and disease progression more faithfully recapitulates aspects of the human disease provides a viable option for identifying relevant mechanisms of resistance.

Results

Here the authors use a transgenic mouse model of HER2 driven breast cancer to investigate the mechanisms of resistance to AZD8931, a pan-HER family inhibitor which is in clinical development for the treatment of HER2-positive tumours. De novo resistance is associated with loss of the tumour suppressor PTEN while acquired resistance develops through two independent mechanisms. This includes a sub-set of tumours in which induction of epithelial-to-mesenchymal transition (EMT), where tumour cells lose their differentiated epithelial phenotype and acquire a more mesenchymal morphology, is concomitant with a loss of HER2 expression.

Implications and future directions

This study highlights the complexity of resistance mechanisms adopted by small molecule inhibitors by using a mouse transgenic model. The observation that 50% of resistant tumours no longer expressed high levels of membranous HER2 could have a significant impact on future treatments as currently secondary treatments are focused on alternative strategies for targeting HER2 signaling. It is rarely mandatory to re-biopsy tumours at the time of entry into clinical trials, and patients whose tumours no longer express HER2 risk being exposed to the toxicity of treatments that might be anticipated to be ineffective. Furthermore exploiting the molecular differences in

resistant tumours that have undergone EMT may provide new therapeutic options. The data provide a strong rationale for basing therapeutic decisions on the biology of the individual resistant tumour, which may be very different from that of the primary tumour.